Basic Study on Robust Perfect Tracking Control Based on Parameter Estimation Reducing Outlier Effects

Shogo Yamada[*] Student Member, Kota Fujimoto[*] Student Member
Hiroshi Fujimoto[*a)] Senior Member

In control systems where fast and precise operation is required, it is essential to implement control system considering parameter fluctuations, especially if the state of the manufactured object changes in the process. On the other hand, outliers may be included in the measurement values when estimating parameters, and robust control algorithm which can deal with these issues is required. This paper aims to apply the approach of batch least squares, where the parameters are estimated in a setting window based on least squares algorithm, and achieve precision control that is robust to parameter fluctuations and outliers. We adopt Huber and Tukey Regression as the method for parameter regression. The effectiveness of the proposed method is verified in simulation and experiments, and a 12.7% performance improvement is achieved compared to the conventional recursive method.

Keywords: adaptive robust control, recursive least squares, Huber regression, Tukey regression

1. Introduction

Manufacturing industry is supported by high production technology using automated machines. To achieve such high productivity, it is essential to move the tools and tables used in the machine as quickly, and also precisely with an accuracy of less than a micrometer as possible. Machines tools, one of the most popular automated machines as shown in Fig. 1, also require further acceleration and precision improvement to shorten processing time and improve tracking accuracy [(1)].

To improve the response speed of the control system, it is required to implement feedforward (FF) control [(2)~(4)]. Multirate perfect tracking control (PTC) has been proposed to realize zero-error at every sampling period with identified nominal parameters [(5) (6)]. However, in machine tools, the mass of the cutting target and the stage positions change during manufacturing. These disturbances are typically compensated by feedback controllers [(7)(8)]; however, some situations cause large parameter errors of the plant model, which has a significant impact on the performance of the FF controller. To solve this issue, multirate adaptive PTC, where parameter estimation is conducted and controllers are updated based on the estimation, has been proposed [(9)]. However, it happens that the estimated value fluctuates greatly when the outliers are included in the measured values. It is required to perform parameter estimation considering it.

In general, it is essential to accurately estimate the state variables for motion control, and various research has been conducted for a long time. One of the most popular estimation methods is the Kalman filter, which is being practically applied in state estimation for quite a lot of applications, such as spacecraft, robots, and many drive systems [(10)~(12)]. On the other hand, it has been pointed out that the Kalman filter is difficult to apply in systems with disturbances that do not follow a normal distribution. To solve these problems, Moving Horizon Estimation, which estimates the state variables based on the concept of least squares for a certain time width of measurement values, has been proposed [(13)(14)]. This method is widely used for model predictive control in the field of control theory because it is easier to set long time spans compared to other methods [(15)(16)].

Figure 1: Machine tools used in manufacturing field as automated machines [(17)].

In this paper, we aim to apply window-based least squares approach and perform parameter estimation for high-precision control including outliers in measured values. Huber and Tukey regression, rapidly growing method in the field of machine learning, are adopted as optimization methods for parameter estimation, and the tracking performance of the proposed method is verified against conventional adaptive control method with Recursive Least Squares (RLS) through simulations and experiments.

The remainder of the paper is organized as follows. In sec-

a) Correspondence to: fujimoto@k.u-tkyo.ac.jp
[*] The University of Tokyo
5-1-5, Kashiwanoha, Kashiwa, Chiba, 227-8561 Japan

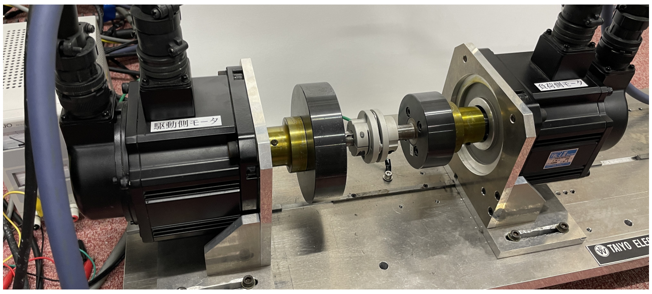

Figure 2: Experimental setups.

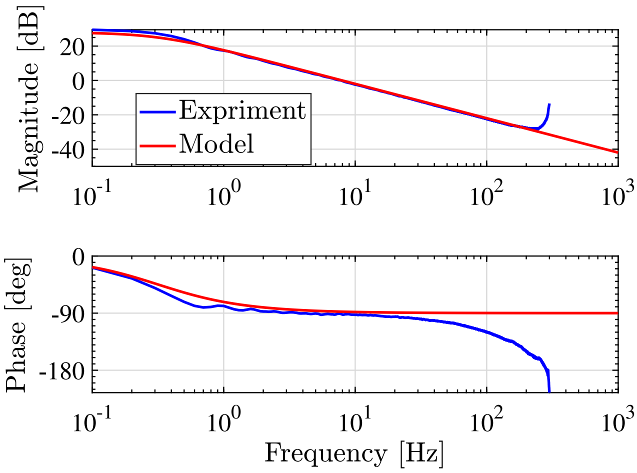

Figure 3: Bode diagram of testbench from drive side motor current to drive side angular velocity.

tion Ⅱ, the nominal model and PTC as the basic FF controller targeted in this paper are introduecd. In section Ⅲ, the proposed estimation method based on Huber and Tukey regression is introduced. In section Ⅳ and Ⅴ, the proposed method is verified through the simulations and experiments. Finally, the paper is concluded in section Ⅵ, with some future studies.

2. Problem Formulation

2.1 Modeling In this paper, the simplest SISO second order system represented by below is considered as a plant model:

$$P = \frac{1}{Js^2 + Ds}. \tag{1}$$

The experiment is conducted using a two-inertia system test bench shown in Fig. 2, by applying the same current in opposite directions to the drive and load side motor to realize Eq.(1) in experimental setups. The drive side motor current is considered as the control input, and the speed of the drive side motor is regarded as the output. The system identification is conducted based on Eq.(1), and determined parameters are shown in Table. 1.

2.2 Perfect Tracking Control In this paper, multirate PTC is adopted as a FF controller to improve the tracking performance. In this section, formulation of PTC is derived.

As mentioned in the previous section, since we are considering a second-order plant this time, the state equation that can be derived from the transfer function of Eq.(1) is given by

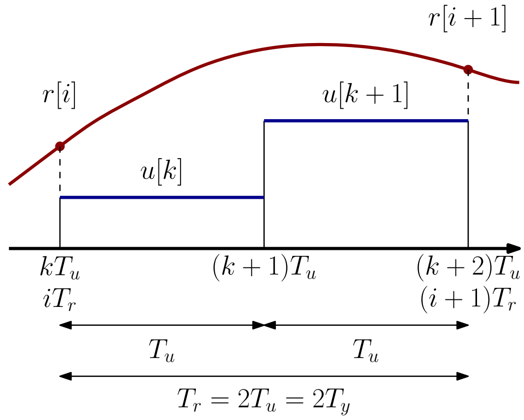

Figure 4: Image diagram of multirate holder for perfect tracking controller.

$$\dot{\boldsymbol{x}}(t) = \boldsymbol{A}_c\boldsymbol{x}(t) + \boldsymbol{b}_c u(t), \tag{2}$$

$$y(t) = \boldsymbol{c}_c\boldsymbol{x}(t) + d_c u(t), \tag{3}$$

$$\boldsymbol{x}(t) = \begin{bmatrix} \theta(t) \\ \omega(t) \end{bmatrix},\ \boldsymbol{A}_c = \begin{bmatrix} 0 & 1 \\ 0 & -D/J \end{bmatrix},$$

$$\boldsymbol{b}_c = \begin{bmatrix} 0 \\ K_t/J \end{bmatrix},\ \boldsymbol{c}_c = \begin{bmatrix} 0 & 1 \end{bmatrix},\ d_c = 0.$$

There are three sampling period, T_r, T_y and T_u, which represents reference period, input period, output period, respectively. Because of the order of the plant is two, the relationship of the three sampling period is $T_r = 2T_y = 2T_u$ as shown in Fig. 4.

The state-space equation discretized at T_u is described as

$$\boldsymbol{x}[k+1] = \boldsymbol{A}_d\boldsymbol{x}[k] + \boldsymbol{b}_d u[k], \tag{4}$$

$$y[k] = \boldsymbol{c}_d\boldsymbol{x}[k] + d_d u[k], \tag{5}$$

$$\boldsymbol{x}[k] = \begin{bmatrix} \theta[k] \\ \omega[k] \end{bmatrix},\ \boldsymbol{A}_d = e^{\boldsymbol{A}_c T_u},\ \boldsymbol{b}_d = \int_0^{T_u} e^{\boldsymbol{A}_c \tau}\boldsymbol{b}_c d\tau.$$

The state-space equation of mulirate plant can be defined as

$$\begin{aligned} \boldsymbol{x}[k+2] &= \boldsymbol{A}_d\boldsymbol{x}[k+1] + \boldsymbol{b}_d u[k+1], \\ &= \boldsymbol{A}_d(\boldsymbol{A}_d\boldsymbol{x}[k] + \boldsymbol{b}_d u[k]) + \boldsymbol{b}_d u[k+1], \\ &= \boldsymbol{A}_d^2\boldsymbol{x}[k] + \begin{bmatrix} \boldsymbol{A}_d\boldsymbol{b}_d & \boldsymbol{b}_d \end{bmatrix} \begin{bmatrix} u[k] \\ u[k+1] \end{bmatrix}. \end{aligned} \tag{6}$$

and Eq.(6) is expressed in time period of T_r as shown in Fig. 4:

$$\begin{aligned} \boldsymbol{x}_d[i+1] &= \boldsymbol{A}\boldsymbol{x}_d[i] + \boldsymbol{B}u[i] \\ \boldsymbol{A} &= \boldsymbol{A}_d^2 \\ \boldsymbol{B} &= \begin{bmatrix} \boldsymbol{A}_d\boldsymbol{b}_d & \boldsymbol{b}_d \end{bmatrix} \end{aligned} \tag{7}$$

Assuming the system is controllable, the multiplicity of the input is equal to the order of the system, so $\boldsymbol{B}$ is regular. Therefore, the control input can be obtained from

$$\begin{aligned} \boldsymbol{u}[i] &= \boldsymbol{B}^{-1}(\boldsymbol{x}_d[i+1] - \boldsymbol{A}\boldsymbol{x}_d[i]) \\ &= \boldsymbol{B}^{-1}(\boldsymbol{I} - z^{-1}\boldsymbol{A})\boldsymbol{x}_d[i+1] \end{aligned} \tag{8}$$

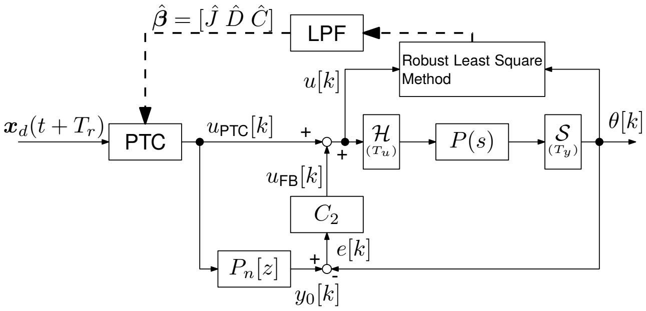

Figure 5: Block diagram of the proposed method.

2.3 Adaptive PTC Using the parameter estimated by RLS [9], or the algorithm described next section, the PTC input corresponding to the time-varying model can be obtained as below with symbols $\hat{\circ}$ as estimation values:

$$\begin{aligned} \boldsymbol{u}[i] &= \hat{\boldsymbol{B}}^{-1}(\boldsymbol{x}_d[i+1] - \hat{\boldsymbol{A}}\boldsymbol{x}_d[i]) \\ &= \hat{\boldsymbol{B}}^{-1}(\boldsymbol{I} - z^{-1}\hat{\boldsymbol{A}})\boldsymbol{x}_d[i+1] \end{aligned} \tag{9}$$

3. Parameter Estimation with Robust Regression

This section outlines parameter estimation algorithm using a robust learning method that is less susceptible to the influence of outliers. Fig. 5 shows a block diagram of the proposed method. The proposed estimation method is applied to get the updated parameters for the adaptive PTC block.

In ordinary least squares, there is a problem that the estimated value becomes strange if there are outliers because it uses l_2 loss. In this study, parameter estimation methods using Huber and Tukey regression, representative methods of robust learning in the field of machine learning, are proposed.

3.1 Huber Regression Huber loss is described as

$$\rho_{\mathrm{Huber}}(r) = \begin{cases} \frac{r^2}{2} & (|r| < \alpha_{\mathrm{Huber}}) \\ \alpha_{\mathrm{Huber}}|r| - \frac{\alpha_{\mathrm{Huber}}^2}{2} & (|r| > \alpha_{\mathrm{Huber}}) \end{cases} \tag{10}$$

where r and α_{Huber} are residual and threshold. Eq.(10) means that if the residual is below the threshold, loss function becomes an l_2 loss, and if it is above the threshold, it becomes an l_1 loss. In other words, when the residual exceeds the threshold, it is considered an outlier and the loss becomes smaller. The learning method using Eq.(10) is Huber loss minimization learning, which is represented as

$$\hat{\boldsymbol{\beta}} = \min_{\boldsymbol{\beta}} J(\boldsymbol{\beta}),\ \ J(\boldsymbol{\beta}) = \Sigma_{i=1}^{n}\rho_{\mathrm{Huber}}(r_i) \tag{11}$$

By using Iterative Reweighed Least Squares learning (IRLS), the following weighted least squares learning can be obtained as a minimization problem for the upper bound.

$$\hat{\boldsymbol{\beta}} = \underset{\boldsymbol{\beta}}{\mathrm{argmin}}\tilde{J}(\boldsymbol{\beta}),\ \ \tilde{J}(\boldsymbol{\beta}) = \frac{1}{2}\Sigma_{i=1}^{n}\omega_i r_i^2 + C \tag{12}$$

where $C = \Sigma_{i:|r_i|>\alpha_{\mathrm{Huber}}}(\alpha_{\mathrm{Huber}}|r_i|/2 - \alpha_{\mathrm{Huber}}^2/2)$ is constant that does not depend on β. The weight ω_i is defined as

$$\omega_i = \begin{cases} 1 & (|r_i| < \alpha_{\mathrm{Huber}}) \\ \frac{\alpha_{\mathrm{Huber}}}{|r_i|} & (|r_i| > \alpha_{\mathrm{Huber}}) \end{cases} \tag{13}$$

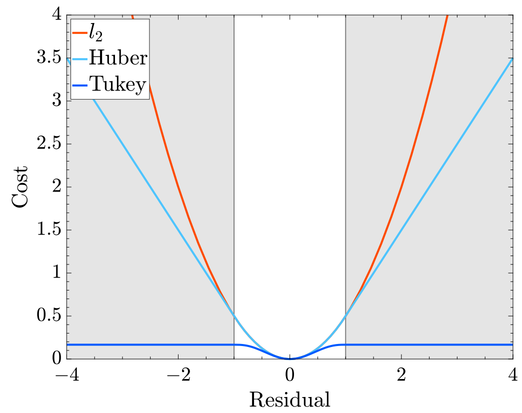

Figure 6: The loss function when the threshold is set to 1.

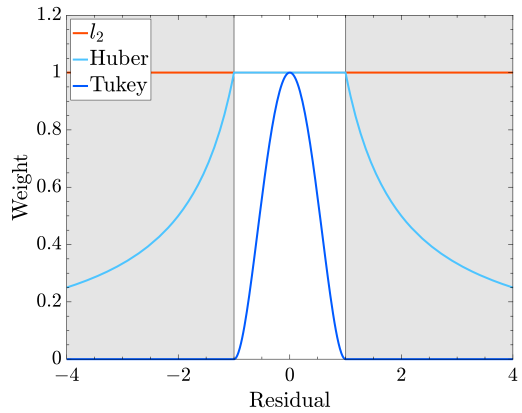

Figure 7: The weight function when the threshold is set to 1.

The solution to the weighted least squares method can be obtained as follows

$$\hat{\boldsymbol{\beta}} = (\boldsymbol{\Phi}^{\mathrm{T}}\boldsymbol{W}\boldsymbol{\Phi})^{-1}\boldsymbol{\Phi}^{\mathrm{T}}\boldsymbol{W}\eta \tag{14}$$

where $W = \mathrm{diag}(\omega_1, \cdots, \omega_M)$ represents the weight matrix. M represents the length of the data for calculation. $\boldsymbol{\Phi}$ is a matrix with M rows and three columns.

3.2 Tukey Regression Tukey loss is described as

$$\rho_{\mathrm{Tukey}}(r) = \begin{cases} (1 - [1 - \frac{r^2}{\alpha_{\mathrm{Tukey}}^2}]^3)\frac{\alpha_{\mathrm{Tukey}}^2}{6} & (|r| < \alpha_{\mathrm{Tukey}}) \\ \frac{\alpha_{\mathrm{Tukey}}^2}{6} & (|r| > \alpha_{\mathrm{Tukey}}) \end{cases} \tag{15}$$

By solving with IRLS in the same way as in the previous section, the weight is given as

$$\omega_i = \begin{cases} (1 - \frac{r^2}{\alpha_{\mathrm{Tukey}}^2})^2 & (|r_i| < \alpha_{\mathrm{Tukey}}) \\ 0 & (|r_i| > \alpha_{\mathrm{Tukey}}) \end{cases} \tag{16}$$

Because of weight ω_i becomes 0 when$|r_i| < \alpha_{\mathrm{Tukey}}$, Tukey regression is completely unaffected by significant outliers.

The loss function and wight function of Huber and Tukey regression is shown in Fig. 6 and Fig. 7 respectively. l_2 means ordinary least square method. In Huber regression, the weight becomes smaller for outliers with large residuals, and in Tukey regression, the weight becomes zero, making estimation robust against outliers.

3.3 Regression Model In this subsection, regression

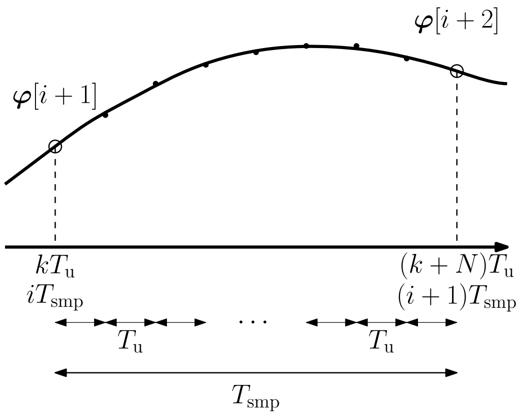

Figure 8: Image diagram of downsampling.

model used in IRLS is given. From Eq.(1), the nominal plant can be modeled as

$$u = J\ddot{\theta} - D\dot{\theta} - C\mathrm{sgn}(\dot{\theta}) \tag{17}$$

where y is the position and C is coulomb friction. Regression model is given by

$$\eta = \boldsymbol{\varphi}^{\mathrm{T}}\boldsymbol{\beta} \tag{18}$$

where $\eta = F(s)$, $\boldsymbol{\varphi}^{\mathrm{T}} = F(s)\begin{bmatrix}\ddot{\theta} & \dot{\theta} & \mathrm{sgn}(\dot{\theta})\end{bmatrix}$ and $F(s)$ is low pass filter for differentiation.

By using $\boldsymbol{\varphi}$, $\boldsymbol{\Phi}$ is represented as

$$\boldsymbol{\Phi} = \begin{bmatrix}\boldsymbol{\varphi}(i+1)\\ \vdots \\ \boldsymbol{\varphi}(i+M)\end{bmatrix} \tag{19}$$

The flow of estimation is as follows. First, determine an appropriate initial value, then calculate the residual and compute the weight matrix, obtain the solution from Eq.(14), and finally, if it converges, update the parameters. To prevent the system from becoming unstable, constraints are set on the range of parameters. The range of constraints is shown in Table. 1.

3.4 Data Sampling To stabilize the estimation, conditional updating is used. If any element of $\boldsymbol{\Phi}$ is close to zero, $\boldsymbol{\Phi}$ is not updated. In addition, to focus on a larger interval, downsampling is performed shown in Fig. 8. Sampling period $T_{\rm smp}$ is larger than control period $T_{\rm u}$.

4. Simulation

In this section, we conduct a simulation to verify the effectiveness of the proposed method. The simulation is conducted on the model represented by Eq.(1). The tracking performance is evaluated for the fifth order polynomial trajectory represented in Fig. 9 when applying PTC, and PTC using RLS as conventional methods, and PTC using Huber regression or Tukey regression as proposed methods. The simulation parameters are as shown in Table. 1. The cutoff frequency of the LPF used for the differentiation calculation is set to 100 Hz. The forgetting factor of the RLS is set to 0.998, aligning the length of the memory horizon with the window length of 500 used in the batch least squares method. The poles of the PID controller are placed at -40π.

Simulations are conducted on the plant which has twice larger inertia than the nominal plant. To observe the impact

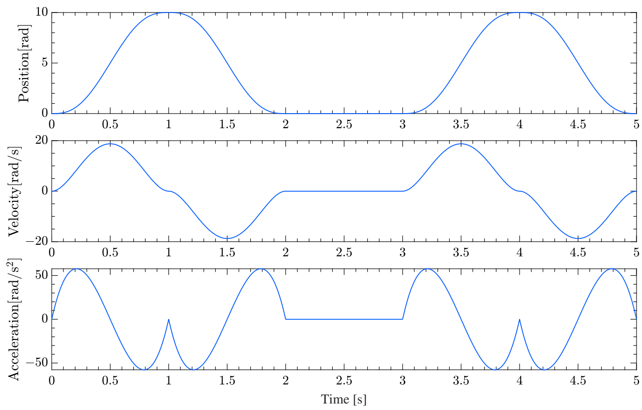

Figure 9: Reference trajectory for simulation (the fifth order polynomial trajectory).

Table 1: Parameters and Settings.

Name	Symbol	Value
Inertia moment	J	2×10^{-2} kgm^2
Viscous Friction Coefficient	D	4×10^{-2} Nms/rad
Coulomb Friction Coefficient	C	0.4 Nm
Torque constant	K_t	1 Nm/A
Input period	$T_{\rm u}$	4×10^{-4} s
Output period	$T_{\rm y}$	4×10^{-4} s
Reference period	$T_{\rm r}$	8×10^{-4} s
Estimation Period	$T_{\rm ls}$	4×10^{-2} s
Sampling Period	$T_{\rm smp}$	4×10^{-3} s
RLS Forgetting Factor(Conv.)	λ	0.998
Data Window Length(Prop.)	M	500
Threshold for Huber Regression	$\alpha_{\rm Huber}$	0.1
Threshold for Tukey Regression	$\alpha_{\rm Tukey}$	0.5
Pole of Closed Loop System		-40π

of outliers on the estimation, a force disturbance of magnitude 0.5 is applied between 1.4 seconds and 1.5 seconds as unmodeled disturbance. Furthermore, assuming a situation where the most significant bit (MSB) is flipped, the sign of the observed value for one sample of 3.5 seconds is reversed. The position, velocity, and acceleration when MSB flips are shown in Fig. 10. Fig. 10 shows that the velocity and acceleration increase instantaneously, resulting in a very large outlier. If the sign of observed value entering the FB controller, the error due to the FB controller becomes too large and the change is difficult to understand, so the outlier is only given to the angle information used for estimation.

The simulation results is shown in Fig. 11 and Fig. 12. Fig. 11 shows the result of RMSE. Fig. 12 shows the results of estimated paramters. Between 1.4 and 1.5 seconds, a force disturbance is added, and the estimated value of RLS is disturbed by the outlier. However, when using Huber regression and Tukey regression, it is found that the estimated value is not much affected. In Huber regression, the RMSE between 0 and 2.5 seconds has increased by 8.1% compared to RLS PTC, and in Tukey regression, it has increased by 8.8%.

From Fig. 12, it is shown that not only RLS but also Huber regression is significantly affected by the large outlier. It is observed that only Tukey regression can estimate without being affected by the outlier. This difference is due to the fact that in Tukey regression, the weight is set to zero for outliers above a certain level, while in Huber regression, the weight only decreases but does not become zero. In Huber regres-

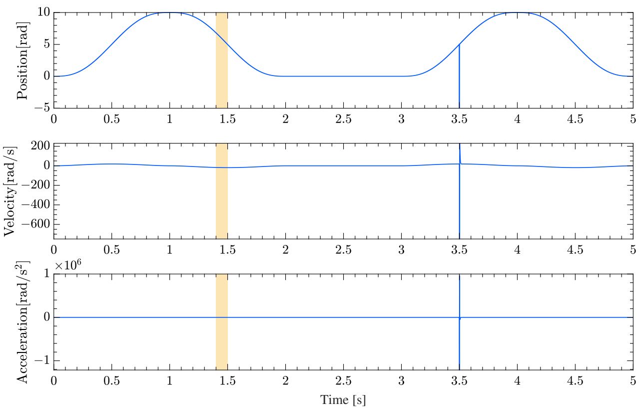

Figure 10: The position, velocity, and acceleration when the sign of observed value reversed. A force disturbance was added where the background is orange.

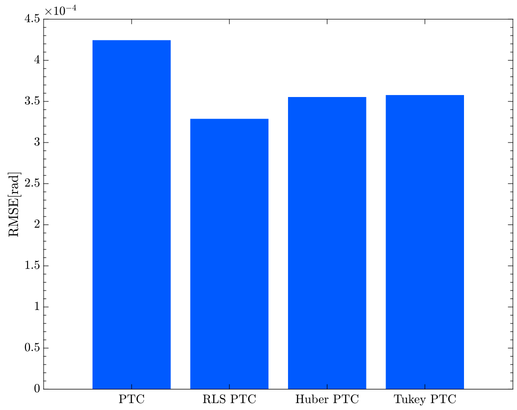

(a) RMSE between 0s and 2.5s.

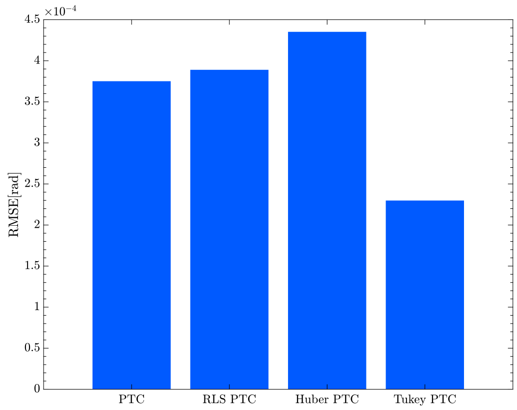

(b) RMSE between 2.5s and 5s.

Figure 11: The RMSE in simulation.

sion, the RMSE between 2.5 and 5 seconds has increased by 11.9% compared to RLS PTC, and in Tukey regression, it has decreased by 41.0%.

These results demonstrate the superiority of the proposed method in the presence of outliers.

5. Experiments

Experiments are conducted on a test bench to verify the effectiveness of the proposed method. To reduce computational load, the calculation of IRLS in the proposed method

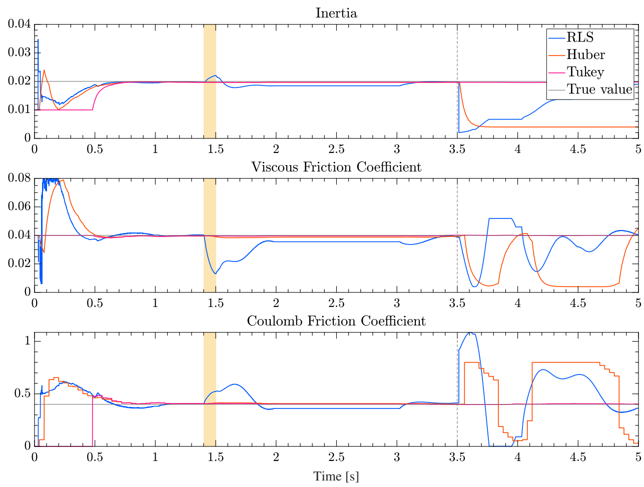

Figure 12: Estimated parameter of simulation.

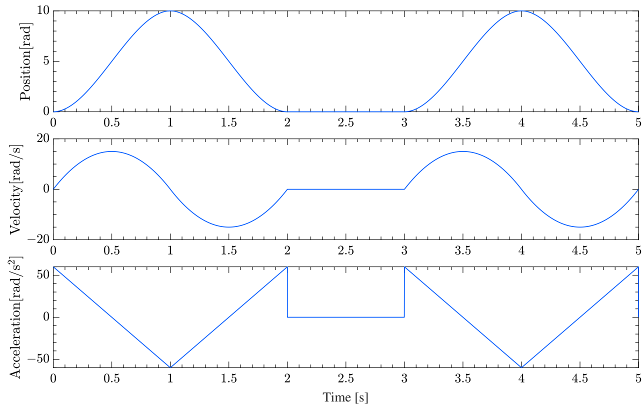

Figure 13: Reference trajectory for experiment (the third order polynomial trajectory).

is performed over a longer period than the control period, prioritizing the calculation of control input and performing matrix calculations for parameter estimation in the remaining time. Due to the computational constraints, the window size used for the calculation of batch least squares in the proposed method is set to 500 and third order trajectory was used shown in Fig. 13.

In the experiment, we conducted the estimation by setting the initial value of the inertia to half of the identified value. In order to make a fair comparison, the inertia of the model used in PTC was also set to half. Similar to the simulation, a force disturbance of magnitude 0.5 was applied between 1.4 seconds and 1.5 seconds and the sign of the observed value for one sample of 3.5 seconds was reversed.

The experimental results is shown in Fig. 14 and Fig. 15. Looking at the RMSE values shown in Fig. 14, the tracking performance of PTC deteriorates due to the parameter error in the model used for PTC. Similar to the simulation, parameters estimated by RLS was affected by outliers. In the proposed method, estimated parameters was less affected by outliers than RLS, and it was confirmed that the RMSE is also small. Huber and Tukey regression could estimate without being affected by a force disturbance. In Huber regression, the RMSE between 0 and 2.5 seconds has decreased by 23.6% compared to RLS PTC, and in Tukey regression, it has

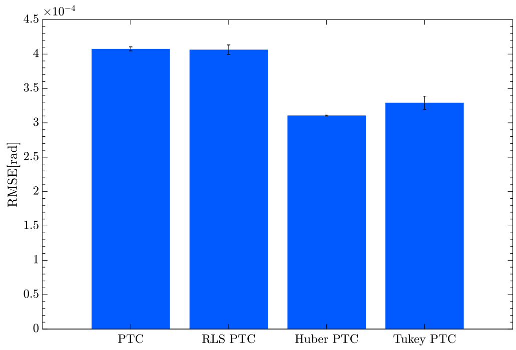

(a) RMSE between 0s and 2.5s.

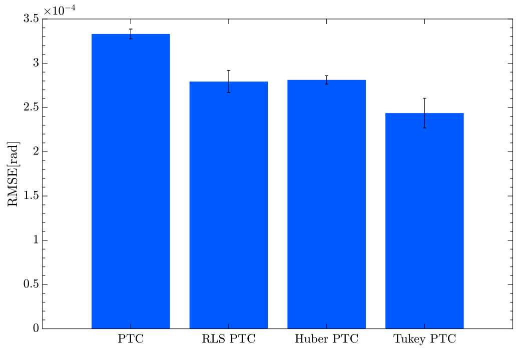

(b) RMSE between 2.5s and 5s.

Figure 14: The average of RMSE of experiment conducted five times.

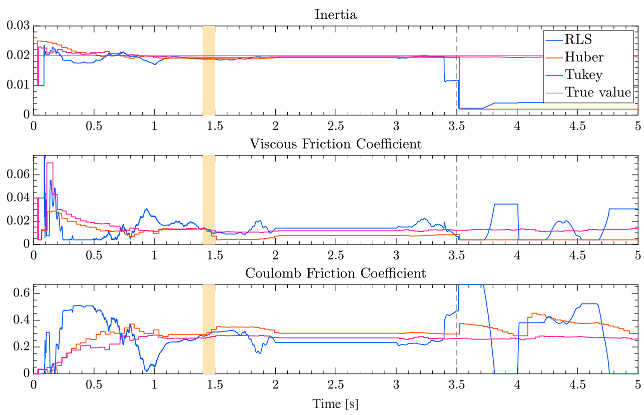

Figure 15: Estimated parameter of experiment.

decreased by 19.0%.

From Fig. 15, when the sign of observed value was reversed, the paramter estimation by Huber regression results in a large error as in the simulation. It is also confirmed from the experiment that Tukey regression is a more effective method when outliers are large. In Huber regression, the RMSE between 2.5 and 5 seconds has increased by 6.8% compared to RLS PTC, and in Tukey regression, it has decreased by 26.8%. In total, RMSE has decreased by 12.7% in Tukey regression.

6. Conclusion

In this paper, a high-performance control algorithm with parameter estimation based on Huber and Tukey regression, which is effective when outliers are included in the measurement values, was proposed. The effectiveness of the proposed method was verified by experiments, and a 12.7% performance improvement is confirmed compared to conventional methods. In future research, comparative studies with other robust methods and detailed considerations on the conditions of PE will need.

References

(1) Y. Altintas, A. Verl, C. Brecher, L. Uriarte, and G. Pritschow, "Machine tool feed drives," *CIRP Annals*, vol. 60, no. 2, pp. 779–796, 2011.

(2) M. Mae, W. Ohnishi, and H. Fujimoto, "MIMO multirate feedforward controller design with selection of input multiplicities and intersample behavior analysis," *Mechatronics*, vol. 71, p. 102442, nov 2020.

(3) M. Poot, J. Portegies, N. Mooren, M. van Haren, M. van Meer, and T. Oomen, "Gaussian processes for advanced motion control," *IEEJ Journal of Industry Applications*, vol. 11, no. 3, pp. 396–407, 2022.

(4) L. Aarnoudse, J. Kon, W. Ohnishi, M. Poot, P. Tacx, N. Strijbosch, and T. Oomen, "Control-relevant neural networks for feedforward control with preview: Applied to an industrial flatbed printer," *IFAC Journal of Systems and Control*, vol. 27, p. 100241, mar 2024.

(5) H. Fujimoto, Y. Hori, and A. Kawamura, "Perfect tracking control based on multirate feedforward control with generalized sampling periods," *IEEE Transactions on Industrial Electronics*, vol. 48, no. 3, pp. 636–644, 2001.

(6) Y. Maeda and M. Iwasaki, "Empirical transfer function estimation with differential filtering and its application to fine positioning control of galvano scanner," *IEEE Transactions of Industrial Electronics*, vol. 70, no. 10, pp. 10466–10475, 2023.

(7) S. Nagao, Y. Kawai, Y. Yokokura, K. Ohishi, and T. Miyazaki, "Load-side acceleration control based on single inertialization compensator and jerk observer for industrial robots," *IEEJ Journal of Industry Applications*, vol. 12, no. 6, pp. 1034–1045, 2023.

(8) J. Padron, K. Tatsuda, K. Ohishi, Y. Yokokura, and T. Miyazaki, "Individual axis control for industrial robots by posture-variant dynamic compensation and feedback control using the FDTD method," *Advanced Robotics*, vol. 38, no. 1, pp. 29–47, 2024.

(9) H. Fujimoto and B. Yao, "Multirate adaptive robust control for discrete-time non-minimum phase systems and application to linear motors," *IEEE/ASME Transactions on Mechatronics*, vol. 10, no. 4, pp. 371–377, 2005.

(10) R. Liu, M. Liu, G. Duan, and X. Cao, "Robust adaptive smooth variable structure kalman filter for spacecraft attitude estimation," *Aerosp. Sci. Technol.*, vol. 144, p. 108784, jan 2024.

(11) R. A. B. Petrea, R. Oboe, and G. Michieletto, "Safe high stiffness impedance control for series elastic actuators using collocated position feedback," *IEEJ Journal of Industry Applications*, vol. 12, no. 4, pp. 735–744, 2023.

(12) K. Szabat, K. Wróbel, and S. Katsura, "Application of multilayer kalman filter to a flexible drive system," *IEEJ Journal of Industry Applications*, vol. 11, no. 3, pp. 483–493, 2022.

(13) G. Zimmer, "State observation by on-line minimization," *Int. J. Control*, vol. 60, pp. 595–606, oct 1994.

(14) A. Alessandri and M. Awawdeh, "Moving-horizon estimation with guaranteed robustness for discrete-time linear systems and measurements subject to outliers," *Automatica*, vol. 67, pp. 85–93, may 2016.

(15) L. Zhang, J. Xie, and S. Dubljevic, "Tracking model predictive control and moving horizon estimation design of distributed parameter pipeline systems," *Comput. Chem. Eng.*, vol. 178, p. 108381, oct 2023.

(16) K. M. Balla, C. Schou, J. D. Bendtsen, C. Ocampo-Martinez, and C. S. Kallesøe, "A nonlinear predictive control approach for urban drainage networks using Data-Driven models and moving horizon estimation," *IEEE Trans. Control Syst. Technol.*, vol. 30, pp. 2147–2162, sep 2022.

(17) DMG MORI, "INH 80." https://www.dmgmori.co.jp/en/products/machine/id=6821. (Accessed on 01/26/2024).